

# Photochemical processes: potential energy surface topology and rationalization using VB arguments

Michael A. Robb<sup>a,\*</sup>, Massimo Olivucci<sup>b,1</sup>

<sup>a</sup> Department of Chemistry, King's College London, Strand, London WC2R 2LS, UK

<sup>b</sup> Dipartimento di Chimica, Università degli Studi di Siena, Via Aldo Moro, I-53100 Siena, Italy

Received 22 December 2000; received in revised form 28 February 2001; accepted 2 March 2001

## Abstract

The development of quantum chemical methods capable of treating excited and ground states of organic molecules in a balanced way has prompted many applications in the field of mechanistic organic photochemistry. In this paper, we review a few representative computational results which illustrate the currently emerging concept of a photochemical (and photophysical) reaction pathway. In particular, we focus on the shape (topology) of the potential energy surface along the excited state branch of the reaction path as well as on the shape and nature of the photochemical funnel where decay to the ground state occurs. The chemical effect of different topologies and their origin in terms of simple valence bond ideas are discussed. © 2001 Published by Elsevier Science B.V.

**Keywords:** Photochemistry; Reaction mechanism; Conical intersection; Computational chemistry

## 1. Introduction

In photochemical processes (for some recent theoretical reviews see [1–4]), the reactant resides on an excited state potential energy surface and the product accumulates on the ground state. Thus, the reaction path must have at least two branches: one located on the excited state potential energy surface and the other located on the ground state potential energy surface. In general, these branches are connected via a “funnel” [5–8] where the excited state reactant or intermediate is delivered to the ground state. The goal of theoretical and computational approaches, in the study of photochemical mechanisms, is the description of what happens at the molecular level from energy absorption to product formation [8]. This involves the description of the reaction co-ordinate from the Franck–Condon (FC) point, located on the potential energy surface of the spectroscopic state, to the photo-product energy valley located on the ground state potential energy surface.

In this paper, we review some of our recent work where the reaction path has been mapped out for photochemical pathways of interest in both chemical physics (where de-

tailed results from time-resolved spectroscopy are available) and in organic chemistry (where, usually, detailed product analysis data are available). We will focus on the conceptual basis of the subject (the way in which the topology of the potential energy surface can control reactivity). We will also show that the computed potential energy surface structure can be rationalized (or sometimes predicted) in terms of simple valence bond arguments. We begin with a brief summary of the theoretical methods that can be used for computational studies of excited state problems.

## 2. Modeling photochemical and photophysical processes

The tools for modeling excited state processes have been developed over the last 10 years and are now available in standard quantum chemistry packages. Space limitations in this paper preclude a detailed discussion and we refer the reader to our recent review [3,4] for a more complete survey. Accordingly, we will limit our discussion to a brief mention of those methods that we have developed and which are distributed as part of standard software, such as the Gaussian package [9]. Since one needs a balanced representation of ground and excited states, standard methods, such as RHF, MP2 and DFT are, in general, not applicable. Methods, such as CASSCF [10] and multi-reference perturbation methods [11,12] (CAS-MP2, CASPT2 and MS-CASPT2) are essen-

\* Corresponding author. Tel.: +44-20-7848-2098; fax: +44-20-7848-2810/2284.

E-mail addresses: mike.robb@kcl.ac.uk (M.A. Robb), olivucci@unisi.it (M. Olivucci).

<sup>1</sup> Tel.: +39-577-234274/80; fax: +39-577-234278.

64 tial. Using these methods, the excited and ground state re- 93  
 65 action paths can be mapped out and the reaction energetics 94  
 66 can be predicted with a level of accuracy that allows com- 95  
 67 parison with the experiment. The new tools required for in- 96  
 68 vestigation of photochemical reaction paths (mainly based 97  
 69 on the use of CASSCF gradients) relate to: 98

- 70 1. Characterizing the potential energy region of the “pho- 99  
 71 tochemical funnel” — the key mechanistic element of 100  
 72 photochemical reactions [13]. This is accomplished by 101  
 73 locating and optimizing the structure of the conical in- 102  
 74 tersections (CI) and singlet/triplet crossings (STC) asso- 103  
 75 ciated to this entity. 104
- 76 2. Locating reaction paths departing from the FC point or 105  
 77 from the CI point [14]. 106
- 78 3. On-the-fly dynamics studies that follow the evolution of 107  
 79 the system according to Newtonian dynamics using the 108  
 80 gradient of the electronic wavefunction (see, for example 109  
 81 [15–17]). 110

### 82 3. How does potential surface topology control 111 83 photochemical and photophysical processes? 112

84 Photochemical or photophysical transformations are 113  
 85 non-adiabatic processes. The reaction co-ordinate begins 114  
 86 on the excited state reached after photoexcitation and ter- 115  
 87 minates on the ground state. The reaction co-ordinate must 116  
 88 thus comprise one or more points where a radiationless (or 117  
 89 non-adiabatic) event occurs and the system decays from 118  
 90 an upper potential energy surface to a lower potential en- 119  
 91 ergy surface. In certain cases, this point occurs after the 120  
 92 bond-breaking/bond-making processes characterizing the 121  
 122

123 reaction have been completed. In this case the photochemi- 124  
 125 cal reaction is “adiabatic” in the sense that it occurs entirely 125  
 on a “single” excited state potential energy surface. How-  
 ever, in other cases the bond-breaking/bond-making process  
 occurs in correspondence of the decay and is characterized  
 by the topology, molecular and electronic structure of the  
 funnel. When the excited and ground state have the same  
 spin multiplicity this funnel corresponds to a CI. On the  
 other hand, when the excited and ground state have dif-  
 ferent spin multiplicity (e.g. triplet and singlet), the funnel  
 corresponds to a crossing (e.g. a singlet triplet crossing  
 STC). Some of the possibilities are illustrated in Fig. 1.

In general, the evolution of the excited state reactant  
 depends on the topology of the funnel and the topology of the  
 excited state potential energy surface. For instance, a conical  
 intersection can be “peaked” as shown in Fig. 1a, b, d  
 and f or “sloped” as shown in Fig. 1c and e. If there is no  
 barrier in the reaction co-ordinate on  $S_1$  (Fig. 1b, d, e and f)  
 then the reaction may be ultrafast. Such processes are can-  
 didates for study using femtochemical methods. They can  
 also be modeled with on-the-fly dynamics. If there is a bar-  
 rier on the reaction co-ordinate (Fig. 1a and c) then the ex-  
 cited state process is activated and one may observe temper-  
 ature or wavelength dependent photochemistry. The sloped  
 conical intersection topology (Fig. 1c) is interesting. Reach-  
 ing the surface crossing is not really an activated process of  
 the type normally encountered in thermochemistry. Even if  
 there is sufficient energy to access the surface crossing, the  
 system may oscillate between excited and ground states in  
 the crossing region for some considerable time before decay  
 to the ground state occur. The rate of the reaction may  
 thus be slower than that predicted on the basis of the energy  
 barrier. This is in contrast to the peaked intersection where,

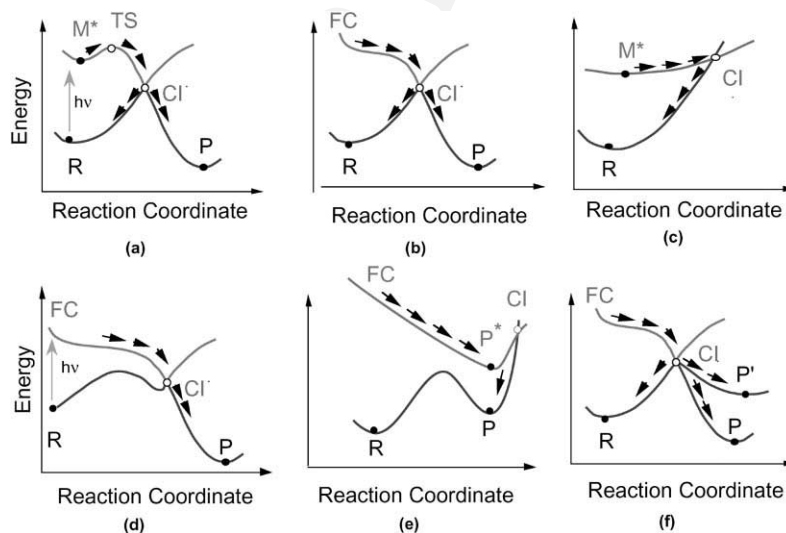


Fig. 1. Schematic representation of the reaction path topology and position of the photochemical funnel (a conical intersection) along the reaction co-ordinate: (a) Transition state (TS) before a peaked conical intersection; (b) barrierless path with a peaked conical intersection; (c) path with a sloped conical intersection; (d) as for a or b but with an intersection on the product side of the reaction co-ordinate; (e) as for c but with an intersection on the product side of the reaction co-ordinate; (f) as for a or b but with multiple competitive ground state relaxation paths.

126 once the crossing is reached, decay to the ground state takes  
127 place on a time scale of less than a vibration.

128 The process of photoproduct formation is affected by the  
129 position of the funnel along the reaction co-ordinate and  
130 the number and orientation of the ground state relaxation  
131 paths departing near the funnel (these paths define ground  
132 state valleys that originate at the CI and end at a differ-  
133 ent photoproduct energy minima). One can see that if the  
134 conical intersection occurs on the product side of the reac-  
135 tion co-ordinate (Fig. 1d and e), one has an excited state  
136 adiabatic reaction which can be substantially completed be-  
137 fore the non-adiabatic event occurs returning the system to  
138 the product region. In this case, the reaction rate may be  
139 controlled by an excited state energy barrier (not shown  
140 in Fig. 1d–e). Provided, there is a substantial thermal bar-  
141 rier to the thermal back reaction then one can have an en-  
142 hanced product yield. Topologies of the form Fig. 1d and  
143 e can be important for photochromism. In different cases,  
144 multiple ground state relaxation paths have been located  
145 departing from the same peaked CI which leads to differ-  
146 ent photoproducts (see Fig. 1f for the case of two competi-  
147 tive product formation paths leading to P and P'). In these  
148 cases two or even more photoproducts could be formed start-  
149 ing from a single excited state reaction co-ordinate. The  
150 presence of a transition state on the  $S_1$  surface provides a  
151 “bottleneck” which can result in an enhanced flux in the  
152 direction of one particular photoproduct. In fact, provided  
153 that the conical intersection and the product lie in the same  
154 “direction”, then the production of product will be enhanced.  
155 We shall return to illustrate these ideas with some examples  
156 subsequently. But first it is useful to discuss the origin of  
157 funnels.

#### 4. Rationalization of potential surface topology using VB arguments

158 Many of the funnels that we have been able to docu-  
159 ment can be understood on the basis of simple VB argu-  
160 ments. Here we also try to make a qualitative connection  
161 with the companion article of Haas and co-workers in this  
162 same workshop issue.  
163

164 We shall try to illustrate the main ideas by classifying,  
165 loosely, conical intersections into four types (there are surely  
166 more, but many of the examples we have studied fall into  
167 these classes).  
168

- 169 1. Three electron  $H_3$ -like triangle.
- 170 2. *Trans*-annular  $\pi$  bonds.
- 171 3. Charge-transfer (e.g. TICT).
- 172 4. The  $n-\pi^*$  re-coupling.

173 This classification provides the guideline to predict the  
174 structure of different conical intersections. We begin with  
175 a brief discussion of type 1–4 and then in a subsequent  
176 section we shall discuss the position and the origin of conical  
177 intersections with some examples.

178 In Fig. 2, we show the characteristic three electron  $H_3$ -like  
179 (type 1) conical intersection that is typical of polyenes [18],  
180 benzenes [19] and other hydrocarbons (see, for example  
181 [20]). This type of conical intersection also provides an op-  
182 portunity to discuss some general ideas about conical inter-  
183 sections. In the  $H_3$ -like (type 1) conical intersection there  
184 are three electrons in an approximately triangular arrange-  
185 ment with a fourth electron acting as a spectator and resid-  
186 ing in a fragment  $\pi$ -orbital (e.g. an allyl, pentadienyl, etc. frag-  
187 ment). In polyenes, the triangular fragment at the center of

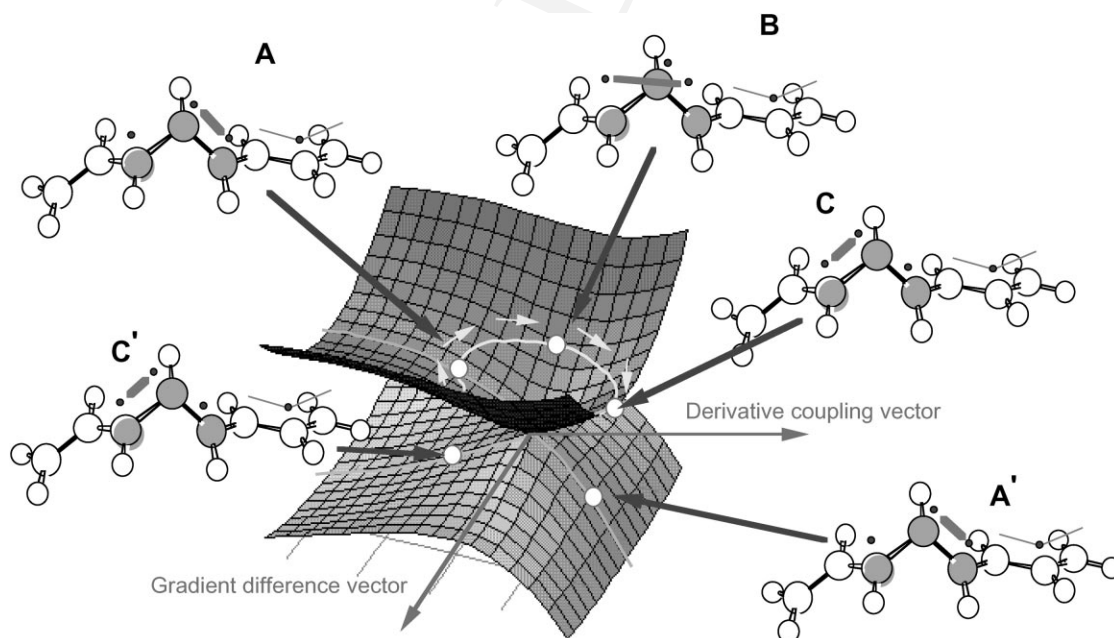


Fig. 2. The VB structures for an  $H_3$ -like conical intersection in a hydrocarbon chain (the position of the corresponding “kink” is indicated by shaded atoms).

188 the conical intersection structure corresponds to a kink lo-  
 189 cated along the chain (see Fig. 2). In general, there are two  
 190 molecular modes (parallel to the derivative coupling and gra-  
 191 dient difference vectors between the upper and lower states)  
 192 that lift the upper state/lower state degeneracy. In type 1,  
 193 conical intersection the degeneracy remains for geometric  
 194 distortions orthogonal to these directions, so that the “point”  
 195 in Fig. 2 becomes a hyperline (a  $f-2$  dimensional space  
 196 where  $f$  is the number of vibrational degrees of freedom of  
 197 the molecule) in  $f$  dimensions. The gradient difference is  
 198 “quasi-totally symmetric” while the derivative coupling is  
 199 “quasi-non-totally symmetric”. Thus, moving along the gra-  
 200 dient, difference directions preserves the approximate  $C_{2v}$   
 201 structure of the triangle while movement along the derivative  
 202 coupling direction retains only approximate  $C_s$  symmetry.  
 203 There are two linearly independent VB couplings of three  
 204 electrons in three orbitals. These are indicated as A and B in  
 205 Fig. 2. VB structure C is a linear combination of A and B.  
 206 As one moves on a circle (see arrows in Fig. 2), remaining  
 207 on the upper surface, the VB coupling changes  $A \rightarrow B \rightarrow$   
 208  $C$  through the linear combinations of the two linearly inde-  
 209 pendent VB couplings of three electrons in three orbitals.  
 210 Moving from the left of the upper surface (A) through to the  
 211 right of the lower surface ( $A'$ ), one preserves the VB cou-  
 212 pling. This VB coupling provides the force field that drives  
 213 the geometrical change. These ideas have been used recently  
 214 by Haas in an attempt to predict the photochemical behavior  
 215 from ground state surface topology. For  $H_3$  itself, the infor-  
 216 mation needed for what Haas calls “anchor points” would  
 217 be the three possible degenerate  $H_2 + H$  pairs. These pairs  
 218 can be related to the three different spin coupling schemes  
 219 discussed above. The three pairs would correspond to the

220 anchor points of a Haas diagram, and the equilateral trian-  
 221 gle conical intersection will be confined within these three  
 222 nodes. However, in polyenes, the unusual kink structure may  
 223 be completely distorted and not easily related to ground state  
 224 equilibrium structures and intermediates. This is expected  
 225 to diminish the predictive ability of Haas method.

226 When more than four electrons are involved in the  
 227 coupling/re-coupling process at a conical intersection, the  
 228 arguments are less easily stated. However, conical intersec-  
 229 tions in bicyclic  $\pi$  electron systems can still be qualitatively  
 230 understood. Azulene [21] provides an example of type 2  
 231 system and involves a sloped conical intersection and the  
 232 reaction path topology of Fig. 1b. The ground state is a  
 233 delocalized system with a *trans*-annular single bond (see  
 234 Fig. 3a). In the excited state, one has a biradical structure  
 235 (Fig. 3b) with a *trans*-annular double bond. Compressing  
 236 the *trans*-annular single bond from the ground state ( $S_0$ )  
 237 equilibrium value drives the  $S_0$  energy up steeply while  
 238 it lowers the energy for double bond on the excited state  
 239 ( $S_1$ ). Thus, one reaches the intersection structure shown  
 240 in Fig. 3c along a bond compression co-ordinate. In this  
 241 system the gradient difference mode corresponds to the  
 242 quasi-totally symmetric motion of the *trans*-annular bond  
 243 (Fig. 3d) while the non-totally symmetric derivative cou-  
 244 pling mode (Fig. 3e) is the motion that moves towards the  
 245 localized VB structures of the ring.

246 Type 3 conical intersections (i.e. the charge transfer type)  
 247 are ubiquitous. The polymethine cyanine dyes in Fig. 4a is a  
 248 simple example [22], while biological chromophores, such  
 249 as the different homologues of the retinal protonated Schiff  
 250 (PSBs) base is another example that has been documented  
 251 in detail [23]. For cyanines and PSBs, the conical intersec-

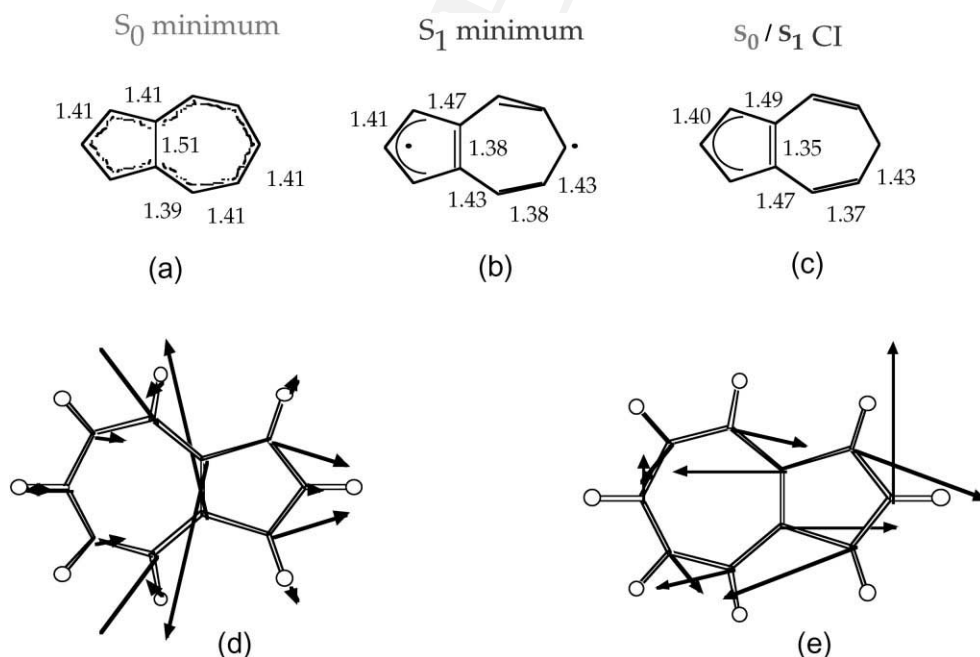


Fig. 3. Azulene conical intersection: (a–c) molecular geometries and VB structures; (d) gradient difference vector; (e) derivative coupling vector.

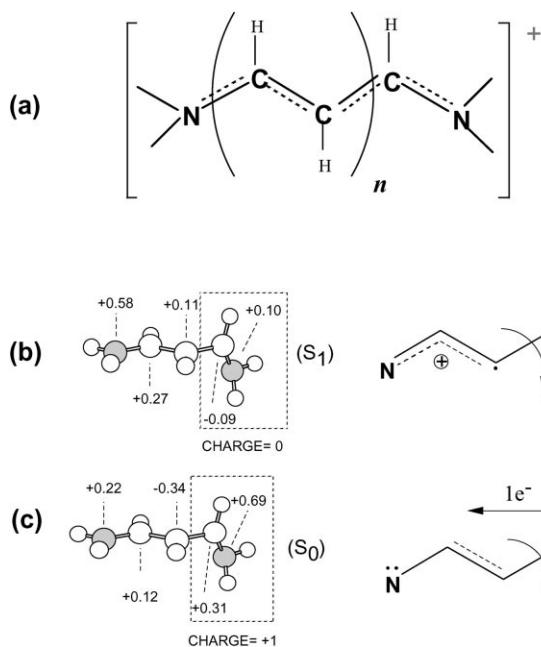


Fig. 4. Conical intersection in cyanines: (a) general structure of polymethine cyanines; (b and c) molecular geometries, VB structures and charges of the trimethine cyanine conical intersection. The total charge of the framed moiety of the molecule is also given.

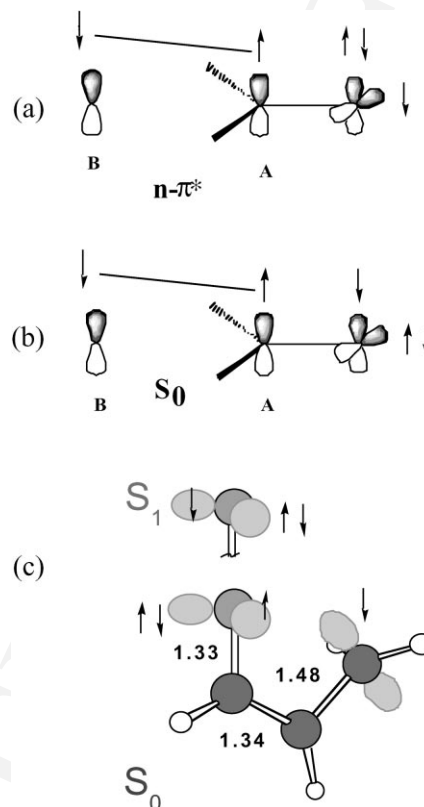


Fig. 5.  $S_0/S_1(n-\pi^*)$  conical intersections: (a and b) schematic VB structures; (c) the example of acrolein.

tion occurs roughly halfway along a *cis-trans*-isomerization co-ordinate at the geometry given in Fig. 4b and c for trimethine cyanine. At this geometry, the ground state  $S_0$  and excited state  $S_1$  cross. The resonance structures for the degenerate  $S_0$  and  $S_1$  states of this model cyanine are shown in the same figures. At the conical intersection geometry these structures correspond to that of a “classic” twisted internal charge transfer (TICT) structure where the two halves of the twisted molecule differ by the charge of one electron. The occurrence of an  $S_0/S_1$  intersection (i.e. an energy degeneracy) can be rationalized on the basis of the fact that these systems correspond to heterosymmetric diradicaloids [24] where the energies of certain frontier orbitals of two weakly interacting moieties are equal. For instance, in our cyanine model containing six  $\pi$ -electrons, the SOMO energy of the  $H_2N-CH-CH-$  moiety taken with three  $\pi$ -electrons and the LUMO energy of the  $-CH-NH_2$  moiety taken with two  $\pi$ -electrons, is equal at the optimized CI structure (see Fig. 4c). As a consequence, the placement of the sixth  $\pi$ -electron on either the moiety (yielding the resonance structures of Fig. 4c and b, respectively) will result in the same stabilization.

Finally, the type 4 conical intersection for  $S_0/S_1(n-\pi^*)$  systems is also easily rationalized. Consider the model system shown in Fig. 5a and b and comprising a carbonyl group interacting with a singly occupied  $p_z$  orbital. When the singly occupied carbonyl carbon  $p_z$  orbital (A in Fig. 5a and b) becomes coupled to that of the adjacent carbon center (B in Fig. 5a,b), and decoupled from the oxygen (O) center,

then the  $(O_{p_z})^1(O_{p_x})^2$  and  $(O_{p_z})^2(O_{p_x})^1$  configurations of the oxygen atom become degenerate in energy. This type of coupling operates in acrolein [25]: the simplest  $\alpha,\beta$ -enone. In Fig. 5c, we report the geometry of the  $S_0/S_1(n-\pi^*)$  conical intersection of acrolein together with the VB couplings for  $S_0$  and  $S_1$  states. The twisted position of the terminal methylene group, allows the formation of a double bond between the remaining (central) two carbons, leaving the O atom isolated. This type of conical intersection can be easily related to the ground state relaxation path and VB recoupling scheme leading to oxetane formation (a four membered heterocyclic compound with one oxygen atom) or even *cis-trans*-isomerization when the  $\alpha,\beta$ -double bond is substituted. In particular, the cyclization involves interaction of the oxygen atom in its  $S_1$  configuration (see Fig. 5c) with the unpaired electron in the terminal  $CH_2$  group and successive C–O bond formation.

## 5. Conclusion

In the preceding two sections, we have revised different systems where the excited state path topology and funnel topology are different. Further, in all cases, the origin of the funnel can be understood using qualitative chemical argu-

Table 1  
Funnel (conical intersection) topologies and their VB models

Reaction or molecule	Reference	Reaction path and funnel topology (Fig. 1)						VB description of the funnel (see text)			
		1a	1b	1c	1d	1e	1f	i	ii	iii	iv
Cyanine	[22]					X				X	
PSB	[23]		X							X	
H <sup>•</sup> transfer	[24]	X								X	
Azulene	[21]			X					X		
Pentalene	[27]			X					X		
Benzene	[19]	X							X		
Cyclohexadiene/hexatriene	[28]						X		X		
β,γ-Enones	[30]				X						X

303 ments related to resonance theory (VB spin coupling argu-  
304 ments). This can be seen as a refinement of the correlation  
305 diagrams that are commonly used in organic photochem-  
306 istry. Our purpose in this section is to summarize these con-  
307 ceptual threads with some examples that are collected in  
308 Table 1.

309 A quick inspection of Table 1 shows that for a set of  
310 selected examples, most combinations of potential surface  
311 topology, conical intersection topology and VB type are  
312 found in practice. Thus, taking the charge transfer CI (type  
313 3) as an example, for the photoisomerization of the proto-  
314 nated Schiff retinal [22], the CI is peaked, and occurs al-  
315 most half way along the isomerization co-ordinate. In con-  
316 trast, for the cyanine systems we have shown [22] that  
317 the conical intersection is sloped and occurs on the prod-  
318 uct side of the barrier. For a hydrogen transfer reaction,  
319 in reference [26], we have shown that the conical intersec-  
320 tion lies almost halfway along the reaction co-ordinate so  
321 that the “adiabatic” photochemical transformation becomes  
322 “aborted” and the reactant may be regenerated. The variabil-  
323 ity observed in the photochemical transformation of unsat-  
324 urated hydrocarbons is large. In these species the VB struc-  
325 ture of the conical intersection is either type 1 or 2. In azu-  
326 lene [21], one has a sloped conical intersection of type 3  
327 so that only a photophysical process (corresponding to ra-  
328 diationless deactivation) is observed. While for the cyclo-  
329 hexadiene/hexatriene system, the intersection is also sloped  
330 but occurs at a geometry where both product formation,  
331 reactant back-formation and, in certain substituted deriva-  
332 tives, bicyclic photoproduct formation is observed (this cor-  
333 responds to the case of Fig. 1f). Benzene [19], has a conical  
334 intersection of type 1, in spite of being an aromatic sys-  
335 tem. The occurrence of a minimum and a transition state  
336 (Fig. 1a) is consistent with the observed wavelength depen-  
337 dent photochemistry. Finally, in  $S_0/n-\pi^*$  systems (type iv),  
338 one also has a considerable variety. In such systems (see  
339 [29]), one also has triplet–triplet ( $T_1/T_2$ ) conical intersec-  
340 tions that occur at the same geometries as the singlet–singlet  
341 ( $S_0/S_1$ ) ones and the potential surface can be very comple-  
342 x (see also the case of the photolysis of azoalkanes in  
343 [30]).

## Acknowledgements

344

A NATO Grant (CRG 950748) finances the collaboration  
between M.A.R. and M.O.

345

346

## References

347

- [1] F. Bernardi, M.A. Robb, M. Olivucci, *Chem. Soc. Rev.* 25 (1996) 348  
321–328. 349
- [2] F. Bernardi, M. Olivucci, J. Michl, M.A. Robb, *The Spectrum* 9  
(1997) 1–5. 350  
351
- [3] M.A. Robb, M. Garavelli, M. Olivucci, F. Bernardi in: K.B. 352  
Lipkowitz, D.B. Boyd (Eds.), *Reviews in Computational Chemistry*,  
Wiley, New York, Vol. 15, 2000, pp. 87–146. 353  
354
- [4] M. Olivucci, M.A. Robb, F. Bernardi in: J. Waluk (Ed.), 355  
*Conformational Analysis of Molecules in Excited States*, Wiley, New  
York, 2000, pp. 297–366. 356  
357
- [5] E. Teller, *Isr. J. Chem.* 7 (1969) 227–235. 358
- [6] H.E. Zimmerman, *J. Am. Chem. Soc.* 88 (1966) 1566. 359
- [7] J. Michl, *Mol. Photochem.* 4 (1972) 243. 360
- [8] W. Fuss, K.L. Kompa, S. Lochbrunner, A.M. Muller, *Chem. Phys.*  
232 (1998) 174. 361  
362
- [9] M.J. Frisch, G.W. Trucks, H.B. Schlegel, P.M.W. Gill, B.G. Johnson,  
M.A. Robb, J.R. Cheeseman, T. Keith, G.A. Petersson, J.A.  
Montgomery, K. Raghavachari, M.A. Al-Laham, V.G. Zakrzewski,  
J.V. Ortiz, J.B. Foresman, J. Cioslowski, B.B. Stefanov, A.  
Nanayakkara, M. Challacombe, C.Y. Peng, P.Y. Ayala, W. Chen,  
M.W. Wong, J.L. Andres, E.S. Replogle, R. Gomperts, R.L. Martin,  
D.J. Fox, J.S. Binkley, D.J. Defrees, J. Baker, J.P. Stewart, M.  
Head-Gordon, C. Gonzalez, J.A. Pople, *Gaussian 94*, Gaussian, Inc.,  
Pittsburgh, PA, 1995. 363  
364  
365  
366  
367  
368  
369  
370  
371
- [10] B.O. Roos, in: K.P. Lawley (Ed.), *Advanced Chemistry and Physics*  
(*Ab Initio Methods in Quantum Chemistry, Part II*), Wiley, New  
York, 1987, Vol. 69, pp. 399–446. 372  
373  
374
- [11] J.J. McDouall, K. Peasley, M.A. Robb, *Chem. Phys. Lett.* 148 (1988)  
183. 375  
376
- [12] K. Andersson, P.A. Malmqvist, B.O. Roos, *J. Chem. Phys.* 96 (1992)  
1218. 377  
378
- [13] M.J. Bearpark, M.A. Robb, H.B. Schlegel, *Chem. Phys. Lett.* 223  
(1994) 269. 379  
380
- [14] P. Celani, M.A. Robb, M. Garavelli, F. Bernardi, M. Olivucci, *Chem.*  
*Phys. Lett.* 243 (1995) 1–8. 381  
382
- [15] M.J. Bearpark, F. Bernardi, S. Clifford, M. Olivucci, M.A. Robb,  
B.R. Smith, *J. Am. Chem. Soc.* 118 (1996) 169–175. 383  
384
- [16] T. Vreven, F. Bernardi, M. Garavelli, M. Olivucci, M.A. Robb, H.B.  
Schlegel, *J. Am. Chem. Soc.* 119 (1997) 12687–12688. 385  
386

- 387 [17] S. Klein, M.J. Bearpark, B.R. Smith, M.A. Robb, M. Olivucci, F. Bernardi, *Chem. Phys. Lett.* 293 (1998) 259–266. 401  
388  
389 [18] M. Olivucci, I.N. Ragazos, F. Bernardi, M.A. Robb, *J. Am. Chem. Soc.* 115 (1993) 3710–3721. 402  
390  
391 [19] I.J. Palmer, I.N. Ragazos, F. Bernardi, M. Olivucci, M.A. Robb, *J. Am. Chem. Soc.* 115 (1993) 673–682. 403  
392  
393 [20] P. Celani, S. Ottani, M. Olivucci, F. Bernardi, M.A. Robb, *J. Am. Chem. Soc.* 116 (1994) 10141–10151. 404  
394  
395 [21] M.J. Bearpark, F. Bernardi, S. Clifford, M. Olivucci, M.A. Robb, B.R. Smith, *J. Am. Chem. Soc.* 118 (1996) 169–175. 405  
396  
397 [22] A. Sanchez-Galvez, P. Hunt, M.A. Robb, M. Olivucci, T. Vreven, H.B. Schlegel, *J. Am. Chem. Soc.* 122 (2000) 2911–2924. 406  
398  
399 [23] M. Garavelli, F. Bernardi, M. Olivucci, T. Vreven, S. Klein, P. Celani, M.A. Robb, *Faraday Discuss.* 110 (1998) 51–70. 407  
400  
[24] J. Michl, V. Bonacic-Koutecky, *Electronic Aspects of Organic Photochemistry*, Wiley, New York, 1990. 408  
[25] M. Reguero, M. Olivucci, F. Bernardi, M.A. Robb, *J. Am. Chem. Soc.* 116 (1994) 2103–2114. 409  
[26] W.M. Nau, G. Greiner, J. Wall, H. Rau, M. Olivucci, M.A. Robb, *Angew. Chem. Int. Ed.* 37 (1998) 98–101. 410  
[27] M.J. Bearpark, F. Bernardi, M. Olivucci, M.A. Robb, *Int. J. Quantum Chem.* 69 (1996) 505–512. 411  
[28] P. Celani, F. Bernardi, M.A. Robb, M. Olivucci, *J. Phys. Chem.* 100 (1996) 19364–19366. 412  
[29] S. Wilsey, M.J. Bearpark, F. Bernardi, M. Olivucci, M.A. Robb, *J. Am. Chem. Soc.* 118 (1996) 176–184. 413  
[30] N. Yamamoto, M. Olivucci, P. Celani, F. Bernardi, M.A. Robb, *J. Am. Chem. Soc.* 120 (1998) 2391–2407. 414